DOE/ET-53088-206 IFSR #206

TWO AND THREE DIMENSIONAL PARTICLE SIMULATION MODELS FOR STUDY OF PLASMA MICROINSTABILITIES

R.D. Sydora, J.N. Leboeuf and T. Tajima
Institute for Fusion Studies
The University of Texas at Austin
Austin, Texas 78712

September 1985

TWO AND THREE DIMENSIONAL PARTICLE SIMULATION MODELS FOR STUDY OF PLASMA MICROINSTABILITIES*

R.D. Sydora, J.N. Leboeuf and T. Tajima
Institute for Fusion Studies
The University of Texas at Austin
Austin, Texas 78712

Abstract

Two and three dimensional particle simulation models suitable for the study of low frequency instabilities in inhomogeneous magnetized plasmas are described. Using the guiding center approximation for electrons transverse to the magnetic field and exact electron dynamics parallel, as well as full ion dynamics, the necessary physics is included to study a class of microinstabilities known as drift waves (the universal mode). Applications of the model to studies of drift wave stability in sheared fields with single and multiple rational surfaces are discussed.

* To appear in "Algorithms, Architectures and the Future of Scientific Computation", edited by T. Tajima and F.A. Matsen, The University of Texas Press.

I. Introduction and Motivation

The most versatile and reliable tools for the study of the many-body properties associated with plasma dynamics and kinetic plasma behavior are the particle simulation techniques.[1] In a conventional particle simulation the Newton-Lorentz equations of motion are advanced in self-consistent fields to obtain velocity and position data from which charge and current densities are collected on a spatial mesh. These densities are then used as sources in Maxwell's equations which determine the self-consistent electric and magnetic fields. The conventional method requires resolution of the fundamental plasma time scale, an electron plasma oscillation and length scale, the Debye length.

In real plasmas phenomena can occur over a wide range of time scales. First a plasma consists of electrons and ions whose time scales are quite different. Secondly, the application of a magnetic field breaks symmetry and introduces anisotropy and separation of time and space scales. For example, low frequency modes primarily propagate in the direction perpendicular to the magnetic field because plasma electrons are more constrained in the perpendicular direction but move freely in the parallel one. In order to enter the regime where low frequency fluctuations dominate the microscopic processes it is necessary to adopt several hybrid approaches. Although the type of model presented in this paper is rather specialized, the approach to modelling other dynamical processes in physical systems may be generalized.

In efficiently describing a magnetized plasma consisting of electrons and ions, it is necessary to modify the electron dynamics if one wishes to study the evolution of the plasma on the ion time scale. One approach[2] is to describe the perpendicular electron dynamics using the guiding-center approximation. Exact dynamics of the electrons is kept parallel to the magnetic field in order to retain wave-particle resonance effects. Full ion dynamics is used in order to include finite ion inertia as well as wave-particle interactions. These have important consequences for low frequency fluctuation stability.

In a three-dimensional plasma model the third dimension along the magnetic field must be included in the equations of motion and in Maxwell's equations. In experimental devices for controlled fusion research such as the tokamak, the axial length is much longer than the transverse dimension ($\gtrsim 10$ times). If the same resolution along the magnetic field is required as across, no computer, presently, could model the plasma. Fortunately, the important collective oscillations associated with plasma confinement have very long wavelengths along the magnetic field line compared to the short wavelengths across. Therefore,

if we perform Fourier expansions in both directions, a fewer number of modes need to be kept in the parallel direction in order to describe the necessary physics. By employing a hybrid approach of eigenfunction expansion along the magnetic field and Fourier expansion on a spatial grid across the magnetic field,[3] we eliminate the problems of aliasing arising from the finite grid length in the parallel direction. This method was first used by Cheng and Okuda in 1977 for modelling drift instabilities in cylindrical and toroidal models.

In the following sections the description of the guiding center particle simulation model used for the study of low frequency microinstabilities is presented. The model is used to investigate low frequency waves excited by plasma inhomogeneities such as drift waves[4] and interchange modes.[5] In toroidal confinement devices the magnetic field lines are twisted or sheared by currents induced in the plasma and this complicates the analysis of these fluctuations. The model presented emphasizes the local global plasma profile. This local approach makes it possible to simulate the structure, perpendicular to the magnetic field, of the microinstabilities. The method of mode selection is used in order to give the correct parity of the fluctuations with respect to the mode rational surfaces ($k_{||} = 0$). In the three dimensional model mode selection, in the z-direction, is used in order to 'fit' the eigenmodes, localized about many different rational surfaces ($k_{||} = 0$, $k'_{||} = 0$, $k''_{||} = 0, \ldots$), within the simulation domain.

II. Particle Simulation Model

For the two-and-one-half ($2 - \frac{1}{2}D$) and three-dimensional (3D) slab models considered here, the magnetic field is oriented in the z-direction with a small y component. Since the low frequency oscillations of interest propagate nearly perpendicular to the magnetic field ($k_\perp >> k_{||}$), the particle motion can be decoupled into components parallel and perpendicular to the magnetic field

$$d\mathbf{x}_\perp/dt = \mathbf{v}_\perp = c\mathbf{E}_\perp \times \mathbf{B}/B^2, \tag{1}$$

$$dv_{||}/dt = q_\alpha E_{||}/m_\alpha \quad ; \quad dx_{||}/dt = v_{||}. \tag{2}$$

Hence, for the electrons, a combination of the second order, time centered, leapfrog scheme for the parallel velocity and displacement and predictor-corrector method for the perpendicular velocities and displacements is used[2]

$$(v_{||}^{n+1} - v_{||}^{n})/\Delta t = -|e|E_{||}^{n+1/2}(\mathbf{x}^{n+1/2})/m_e, \tag{3}$$

$$\mathbf{v}_{\perp}^{n+1/2} = c\big(\mathbf{E}^{n+1/2} \times \mathbf{B}\big)/B^2, \tag{4}$$

$$\big(\mathbf{x}_{\rm pred}^{n+3/2} - \mathbf{x}^{n-1/2}\big)/2\Delta t = \big(v_{\parallel}^{n+1} + v_{\parallel}^{n}\big)/2\hat{e}_{\parallel} + \mathbf{v}_{\perp}^{n+1/2}, \tag{5}$$

$$\mathbf{v}_{\perp}^{n+3/2} = c\big(\mathbf{E}_{\rm pred}^{n+3/2} \times \mathbf{B}\big)/B^2, \tag{6}$$

$$\big(\mathbf{x}_{\rm cor}^{n+3/2} - \mathbf{x}^{n+1/2}\big)/\Delta t = v_{\parallel}^{n+1}\hat{e}_{\parallel} + c\big(\mathbf{E}^{n+1/2} \times \mathbf{B} + \mathbf{E}_{\rm pred}^{n+3/2} \times \mathbf{B}\big)/2B^2. \tag{7}$$

Poisson's equation is solved twice per time step to obtain the electric field.

The ion dynamics can be treated in a similar manner. However, in order to preserve the finite ion Larmor radius effects, the full Newton-Lorentz equation of motion is solved using the leapfrog scheme

$$(\mathbf{v}^{n+1} - \mathbf{v}^{n})/\Delta t = |e|/m_i\big[\mathbf{E}^{n+1/2} + (\mathbf{v}^{n+1} + \mathbf{v}^{n})/2 \times \mathbf{B}/c\big], \tag{8}$$

$$(\mathbf{x}^{n+3/2} - \mathbf{x}^{n+1/2})/\Delta t = \mathbf{v}^{n+1}. \tag{9}$$

The overall scheme proves to be stable for $\max(\omega_{pe}\sin\theta,\ \omega_{pe})\Delta t < 1$, where θ is the angle between the mode propagation and magnetic field directions.

The electric field needed to push the particles is calculated as follows. Consider the three-dimensional slab model shown in Fig. 1. We assume the three-dimensional box is filled with particles of finite size having a Gaussian-shaped form factor

$$S(\mathbf{x} - \mathbf{x}_j) = \big[(2\pi)^{3/2} a_x a_y a_z\big]^{-1} \times e^{(-x-x_j)^2/2a_x^2} e^{-(y-y_j)^2/2a_y^2} e^{-(z-z_j)^2/2a_z^2}, \tag{10}$$

where (x_j, y_j, z_j) is the charge center location and $a_{x,y,z}$ is the particle size in each direction. The charge density is given by

$$\rho(x,y,z) = \sum_{\alpha} \sum_{j} q_{j\alpha}\ S(\mathbf{x} - \mathbf{x}_{j\alpha}), \tag{11}$$

where α denotes the particle species. The finite size particles allow us to simulate collisionless phenomena within realistic computational resources.[1,6]

The normal mode expansion method is applied in the z direction by Fourier analyzing the charge density and potential with respect to z. For the charge density this gives

$$\rho(x,y,z) = \sum_{n=-N}^{N} \rho_n(x,y) e^{ik_z z}, \tag{12}$$

where

$$\rho_n(x,y) = [2\pi\ a_x a_y L_z]^{-1} e^{-k_z a_z^2/2} \times \\ \times \sum_{\alpha} \sum_{j} q_{j\alpha} e^{-(x-x_{j\alpha})^2/2a_x^2} e^{-(y-y_{j\alpha})^2/2a_y^2} e^{-(z-z_{j\alpha})^2/2a_z^2} \tag{13}$$

with L_z the system length in the z-direction ($L_z >> L_x \sim L_y$) and $k_z = 2\pi n/L_z$, $n = 0$, ± 1, ..., $\pm N$. Typically $N = 5 - 20$ is satisfactory for the present problem. The charge density is computed on the two-dimensional spatial grid by using the subtracted dipole scheme (SUDS) of Kruer, Dawson and Rosen.[7] The phase factor, $e^{-ik_z z_{j\alpha}}$, with the exact particle position is left unexpanded because there is no grid in the z-direction.

Mode expanding the potential in the z-direction

$$\left(\phi(x,y,z) = \sum_{n=-N}^{N} \phi_n(x,y) e^{ik_z z}\right),$$

Poisson's equation ($\nabla^2\phi = -4\pi\rho$) becomes

$$\left[\nabla_{xy}^2 - \left(\frac{2\pi n}{L_z}\right)^2\right] \phi_n(x,y) = -4\pi\rho_n(x,y). \tag{14}$$

This is a two-dimensional Poisson's equation to be solved for each mode number in the z-direction. It is done by use of fast Fourier transform (FFT) techniques. Further, the electric field for each mode number n is given by

$$\mathbf{E}_n(k_x,k_y) = -i\mathbf{k}\phi_n(k_x,k_y) = -4\pi i(\mathbf{k}/k^2)\rho_n(k_x,k_y). \tag{15}$$

The electric force on a finite size particle needed to update the particle velocities and positions is computed from

$$\mathbf{F}(k_x,k_y,z_j) = (q_j/m_j) \sum_{n=-N}^{N} e^{-k_z^2 a_z^2/2} e^{ik_z z_j} \mathbf{E}_n(k_x,k_y) e^{-k_x^2 a_x^2/2} e^{-k_y^2 a_y^2/2}. \tag{16}$$

$F(x,y,z_j)$ is calculated from the inverse Fourier transform of Eq. (16) and interpolated to the particle position (x_j, y_j) by using SUDS.

In the 3D and $2 - \frac{1}{2}$ $D(k_z = 0$ limit of the algorithm outlined earlier) models, the slab is bounded in the x-direction and periodic in y and z. The particles are reintroduced in a periodic fashion in the y and z directions and reflected at the boundaries in x according to

the prescription of Naitou et al.[8] The boundary conditions on the charge density, potential and electric fields are handled by the image charge method over twice the system length in the x direction ($2L_x$) by setting

$$\rho_n(2L_x - x, y) = \pm\rho_n(x, y) \tag{17}$$

with the $(+)$ sign dictated by $\frac{\partial \phi}{\partial x} = 0$ at $x = 0$ and $x = L_x$ and the $(-)$ sign by $\phi = 0$ at $x = 0$ and $x = L_x$. The potential and electric fields with the proper parity are directly obtained from Eqs. (14) and (15) with Fourier transform performed over the double system of size $(2L_x, L_y)$. For $\phi = 0$ at the end points, the potential normal modes are expressed as $\tilde{\phi}(x) = \sum_\ell \tilde{\phi}_\ell \sin\left(\frac{\ell \pi x}{L_x}\right)$; for $\phi' = 0$ at the endpoints, they are expressed at $\tilde{\phi}(x) = \sum_\ell \tilde{\phi}_\ell \cos\left(\frac{\ell \pi x}{L_x}\right)$.

For simulations of drift waves in a sheared magnetic field written as $\mathbf{B} = \left(0, B_0 \frac{x - x_0}{L_s},\ B_0\right)$ with L_s the shear length, careful consideration has to be given to the parity of the eigenmodes with respect to the rational surface position x_0 (in 2D). Comparison of simulations with theory further requires that the wave-particle resonance region x_α of each species $(\alpha = e, i)$ defined by $\omega_{*e} \simeq k_{||}(x_\alpha) v_{t\alpha}$, with electron diamagnetic drift frequency $\omega_{*e} = (k_y / L_n) c T_e / eB$, and L_n the density gradient scale length, be within the system and sufficiently away from the endpoints. For $\phi = 0$ at the endpoints and $x_0 = 0$, the drift eigenmodes will have odd parity with respect to the rational surface; for $\phi' = 0$ at the endpoints and $x_0 = 0$, they will have even parity. For $\phi = 0$ or $\phi' = 0$ at the endpoints and $x_0 = L_x/2$, they would have mixed parity. The relevant parity can however be recovered by selecting only the even or odd modes with respect to $x_0 = L_x/2$ in the shape factor $S(k_x, k_y, k_z)$. For instance $\phi = 0$ at the endpoints, so that $\tilde{\phi}(x) = \sum_\ell \tilde{\phi}_\ell \sin\left(\frac{\ell \pi x}{L_x}\right)$, will yield even parity with respect to x_0 if only the odd ℓ numbers are kept and odd parity with respect to x_0 if only the even ℓ numbers are kept. In 3D, with multiple rational surfaces at $x_{mn} = x_0 - \frac{L_y L_s}{L_z} \frac{n}{m}$, the parity is necessarily mixed and all ℓ's are kept with $x_0 = L_x/2$ and $\phi = 0$ at the endpoints.

To insure that the ion resonance layers are within the system, the natural cut-off in the shape factor due to the finite particle size at $k_x a_x = k_y a_y = k_z a_z \gtrsim 1$ is used to conveniently suppress the modes which would violate the $x_i < L_x$ condition. Therefore, the size of the particles can be adjusted to perform mode selection. Alternatively, mode selection in the z-direction, by limiting the number of modes retained in the Fourier sums, can be performed to limit the rational surface distribution.

III. Applications to Drift Waves

The $2-\frac{1}{2}\,D$ and 3D guiding-center electrons, full dynamics ions codes have been applied to a detailed study of drift wave stability in a sheared magnetic field in the presence of a single rational surface ($2-\frac{1}{2}\,D$) and multiple rational surfaces (3D). The single rational surface simulations are carried out to ascertain that linear drift wave eigenmodes are absolutely stable in a magnetic field with shear.[9] The multiple rational surface simulations are performed to test the hypothesis that nonlinear destabilization[10] of drift waves could occur. The electron response is altered by turbulent diffusion of the electrons across multiple rational surfaces due to a combination of shear and random $\mathbf{E}\times\mathbf{B}$ fluctuations. This results in an effective value for $k_{||}$ which destroys the stabilizing influence of the nonresonant electrons in the immediate vicinity of the rational surface.

For the case of a single rational surface, the $2-\frac{1}{2}\,D$ code is run with the following parameters: $L_x\times L_y = 64\Delta\times 32\Delta$, with Δ the unit grid spacing; average density $n_0 = 16$ particles of each species per unit cell; temperature ration $T_e/T_i = 1$; mass ratio $M_i/m_e = 100$; magnetic field strength B_0 such that $\omega_{ce}/\omega_{pe} = 10$. A density gradient $n(x) = n_0 e^{-\kappa x}$ with $\kappa = L_n^{-1} = 0.07$ is imposed in the x-direction; the plasma is uniform in y. The magnetic field, tilted in the $y-z$ plane, is expressed at $\mathbf{B} = \left(0, B_0\frac{x-x_0}{L_x},\ B_0\right)$ with $L_s/L_n = 28$ and $x_0 = 0$ in the present case. Boundary conditions such that $\frac{\partial\phi}{\partial x} = 0$ at $x = 0$ and $x = L_x$ are imposed to insure even parity of the drift eigenmodes with respect to the rational surface. The system supports discrete wavenumbers $k_y\rho_s = 0.49m$, $m = 0$, ±1, ..., $\pm L_y/2$, with the ion sound Larmor radius $\rho_s = 2.5\Delta$. The electron diamagnetic frequency is $\omega_*/\omega_{pe} = 0.0086m$ and the simulations are run up to $\omega_* t = 70$.

According to linear theory (with our simulation parameters), the drift eigenmodes should be stable. Indeed, the time histories of the total electrostatic energy and the energies per each relevant $k_y\rho_s$ modes do not show any increase above the initial thermal level over the length of the run. To determine whether eigenmodes (which have the same frequency at every point in space) do exist in the simulations, we perform an interferogram of the potential fluctuations. First, the potential fluctuations at every grid point in x and for a few $k_y\rho_s$ modes are stored at each time step of the simulation. Then the following correlation is evaluated

$$\phi(x,k_y,\omega_0) = \frac{1}{T}\int_0^T \phi(x,k_y,t)\sin\omega_0 t dt. \tag{18}$$

The frequency ω_0 is varied in intervals of $0.01\omega_*$ between 0 and ω_*. The interferogram of the potential fluctuations with $k_y\rho_s = 0.49$ at $\omega_0/\omega_* = 0.43$ is displayed in Fig. 2

along with the eigenfunction from linear theory obtained with a shooting code which finds the eigenfrequency to be $\omega/\omega_* = 0.33$. Good agreement is found for both the real and imaginary parts of the potential wavefunction. Stable eigenmodes have also been found to agree with linear theory in the simulations for the cases of rational surface $x_0 = L_x/2$ and both even and odd parity with respect to x_0.[4]

The three-dimensional results reported here are run with the following parameters: system size $L_x \times L_y \times L_z = 64\Delta \times 32\Delta \times 6400\Delta$ with ± 5 modes retained in the z direction; $\omega_{ce}/\omega_{pe} = 35$, $M_i/m_e = 500$, $T_e/T_i = 1$; sound Larmor radius $\rho_s = 1.6\Delta$ so that $k_y\rho_s = 0.31m$; $n(x) = n_0 e^{-\kappa x}$ with $n_0 = 16/\Delta^2$ and $\kappa = L_n^{-1} = 0.07$; $L_s/L_n = 28$ and $\omega_*/\omega_{pe} = 0.0042m$. The simulations are run up to $\omega_*(m = 1) \times t = 30$.

The multiple rational surfaces $x_{mn} = x_0 - \frac{L_y L_s}{L_z \rho_s} \frac{n}{m}$, superimposed on the density profile, are displayed in Fig. 3; only modes with $x_i^{mn}(\omega_*) < L_x$ are retained. A criterion for nonlinear destabilization is that the resonant surfaces be so closely packed (hence the strong shear) so that the trapping width of the drift modes centered at x_{mn}, measured at the thermal level, be larger than their separation. Stochastic diffusion of the electrons then results and destabilization is possible. Our measurements of the thermal level indicate that resonance overlap is easily satisfied. A shooting code solution of the nonlinear eigenmode equation[10] indicates that modes with $m = 3, 4$ and 5 can be destabilized whereas modes with $m = 1$ and 2 are stable.

The behavior of the electrons is probed in the following ways. Electron test particles are selected randomly in the vicinity of the mode rational surfaces. Their positions and velocities are stored at each time step. First, the diffusion coefficient of the test particles is measured from their guiding center displacements as

$$D = \lim_{t \to \infty} \sum_{i=1}^{N} \frac{(\Delta x_i)^2}{2Nt}, \tag{19}$$

where Δx_i is the change in position of the guiding center for the i^{th} particle in time t and N is the number of test electrons. The guiding center displacement as a function of time is displayed in Fig. 4. A linear increase indicates diffusion with diffusion coefficient equal to the slope. Second, electron orbits in $(x, v_\parallel)$ space are constructed. They are displayed in Fig. 5 with the open circles representing their initial location and the dotted curves their subsequent location in time. It is clear that particles encountering the overlapping resonances region can excurse large distances in the x direction as shown in Fig. 5a, b, c and e. Particles selected initially outside the overlap region as in Figs. 5d and f show

very little diffusion in x. These particle diagnostics clearly demonstrate that electrons in the vicinity of the mode rational surfaces exhibit the stochastic behavior across rational surfaces needed for destabilization.

Mode analysis has been performed in the following ways. First, the potential fluctuations $\phi(x, k_y, k_z)$ are stored at each time step of the simulation. The time history of the fluctuations for a particular (m, n) mode is recorded after filtering out frequencies $\omega > \omega_*$. Correlations of the fluctuations (without filtering) are carried out as follows

$$C_{mn}(x, \tau) = \frac{1}{T} \int_0^T \phi_{mn}(x, t) \phi^*_{mn}(x, t + \tau) dt \tag{20}$$

and the power spectrum obtained from the Fourier transform of the autocorrelation function $C_{mn}(x, \tau)$ is given by

$$P_{mn}(x, \omega) = \int_0^\tau C_{mn}(x, \tau') e^{i\omega\tau'} d\tau'. \tag{21}$$

Interferograms are also performed according to Eq. 18.

A typical result for mode $m = 1$, $n = 0$ with $k_y \rho_s = 0.32$ is displayed in Fig. 6: the amplitude of the fluctuation versus time in Fig. 6a, real and imaginary parts versus time in Fig. 6b, power spectrum in Fig. 6c and interferogram with eigenfrequency $\omega_0/\omega_* = 0.7$ in Fig. 6d. The real frequency and mode structure in x agree with the nonlinear eigenmode equation solution. From Figs. 6a and b, it is clear that the mode is stable. All other (m, n) pairs retained in the simulation are also stable in this case, whereas theory predicts that modes with $m = 3, 4$ and 5 can become unstable. The apparent discrepancy between the simulation and theory arises as follows. The stable long wavelength modes ($m = 1$ and $m = 2$) are less affected by the nonlinear electron dynamics and provide a sink of energy for the more unstable shorter wavelengths. Simulations with parameters such that the longest wavelength modes are in the unstable regime do indeed show nonlinear instability[11] arising from the nonlinear electron behavior in the resonance overlap region.

IV. Conclusions

Explicit, bounded, electrostatic, finite sized particle simulation models with guiding-center electrons and full dynamics ions have been developed in two and three dimensions to study phenomena in the drift frequency range in slab geometry and with sheared magnetic fields. The 2D models have been successful in recovering the stable drift

eigenmodes predicted by linear theory with a single rational surface.[4] The 3D models exhibit many of the effects of multiple rational surfaces on the electron dynamics needed for nonlinear destabilization of drift waves.[11]

Variants of these codes have also been applied to resistive interchange modes[5] and are currently being used to study current driven drift waves and the ion mixing mode with electron and ion temperature gradients as well as density gradients.

Acknowledgments

This work was supported by the U.S. Department of Energy contract no. DE-FG05-80ET-53088, and the National Science Foundation grant no. ATM-82-14730.

References

1. J.M. Dawson, Rev. Mod. Phys. **55**, 403 (1983).
2. W.W. Lee and H. Okuda, J. Comp. Phys. **26**, 139 (1978).
3. C.Z. Cheng and H. Okuda, J. Comp. Phys. **25**, 133 (1979).
4. R.D. Sydora, J.N. Leboeuf and T. Tajima, Phys. Fluids **28**, 528 (1985).
5. R.D. Sydora, J.N. Leboeuf, Z.G. An, P.H. Diamond and T. Tajima, Phys. Fluids **28**, 425 (1985).
6. R. Hockney and J. Eastwood, Computer Simulations Using Particles (McGraw Hill, New York, 1981).
7. W. Kruer, J.M. Dawson and B. Rosen, J. Comp. Phys. **13**, 114 (1973).
8. H. Naitou, S. Tokuda and T. Kamimura, J. Comp. Phys. **33**, 86 (1979).
9. D.W. Ross and S.M. Mahajan, Phys. Rev. Lett. **40**, 324 (1978).
10. S.P. Hirshman and K. Molvig, Phys. Rev. Lett. **42**, 648 (1979).
11. R.D. Sydora, Ph.D. Thesis, The University of Texas at Austin, 1985.

Figure Captions

Fig. 1 Three-dimensional slab model.

Fig. 2 Density profile and mode rational surface positions.

Fig. 3 Stable 2D linear eigenmode at $\omega_0/\omega_* = 0.43$.

Fig. 4 Guiding-center displacement and diffusion coefficient of resonant electrons.

Fig. 5 Test orbits of the resonant electrons. Strong diffusion: a), b), c) and e). Weak diffusion: d) and f).

Fig. 6 Test wave diagnostics.

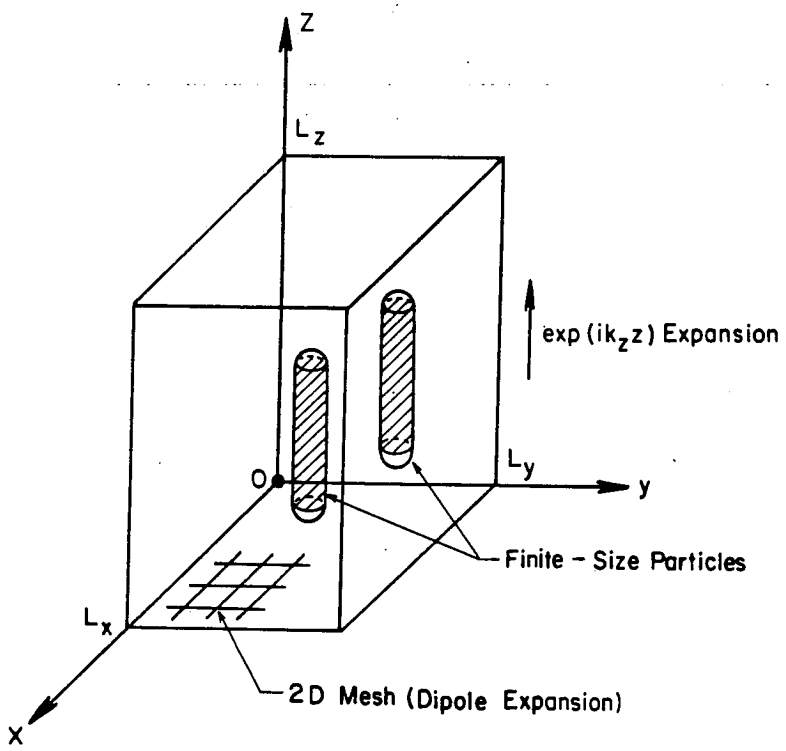
Z
L_z
exp ($ik_z z$) Expansion
L_y
O
y
Finite - Size Particles
L_x
2D Mesh (Dipole Expansion)
X

Fig. 1

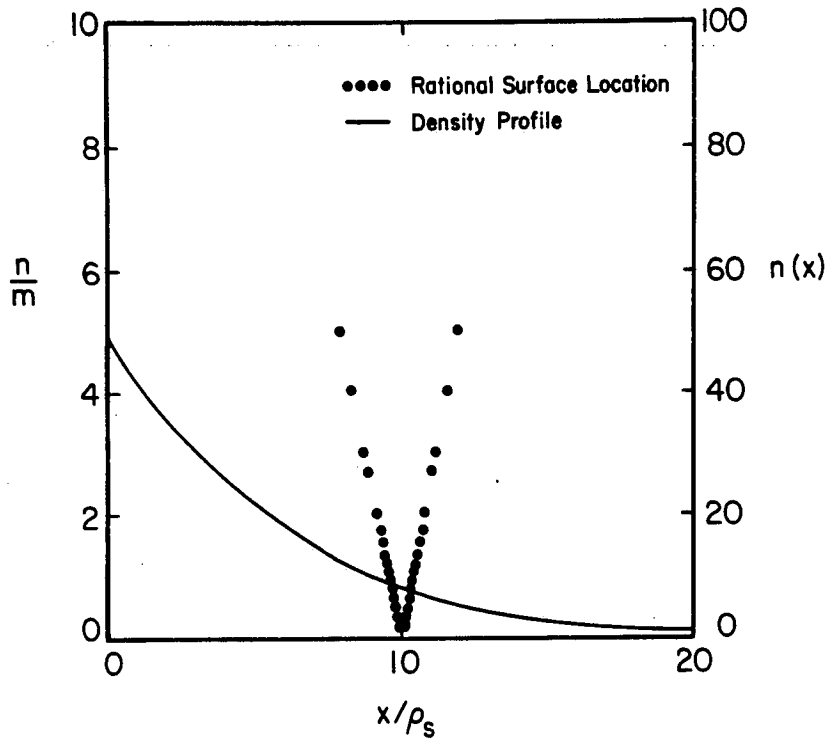
Rational Surface Location
Density Profile
10
8
6
4
2
0
m/n
100
80
60
40
20
0
n(x)
0
10
20
x/ρs

Fig. 2

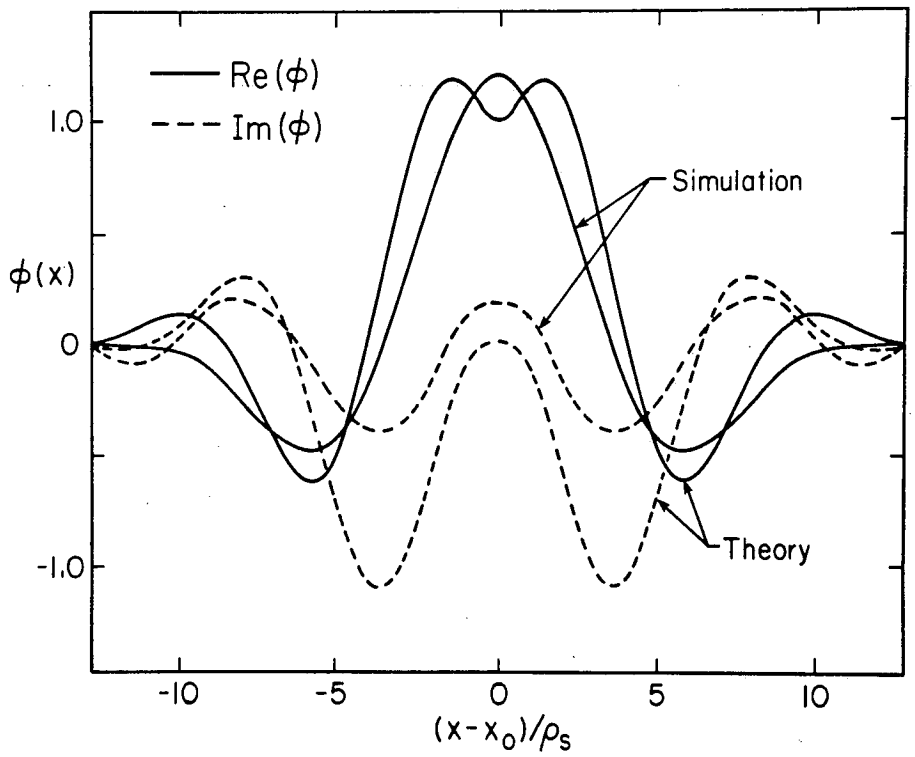

Fig. 3

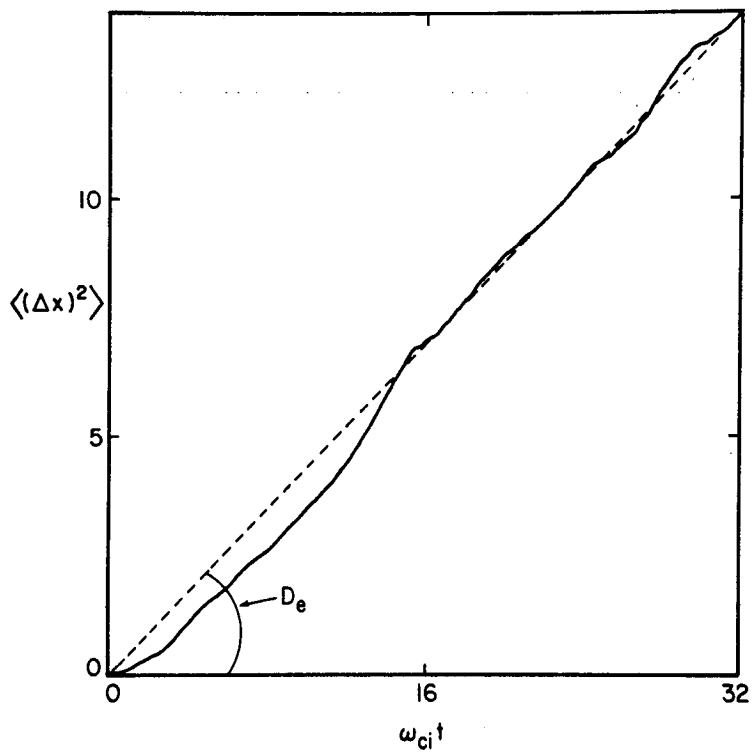

Fig. 4

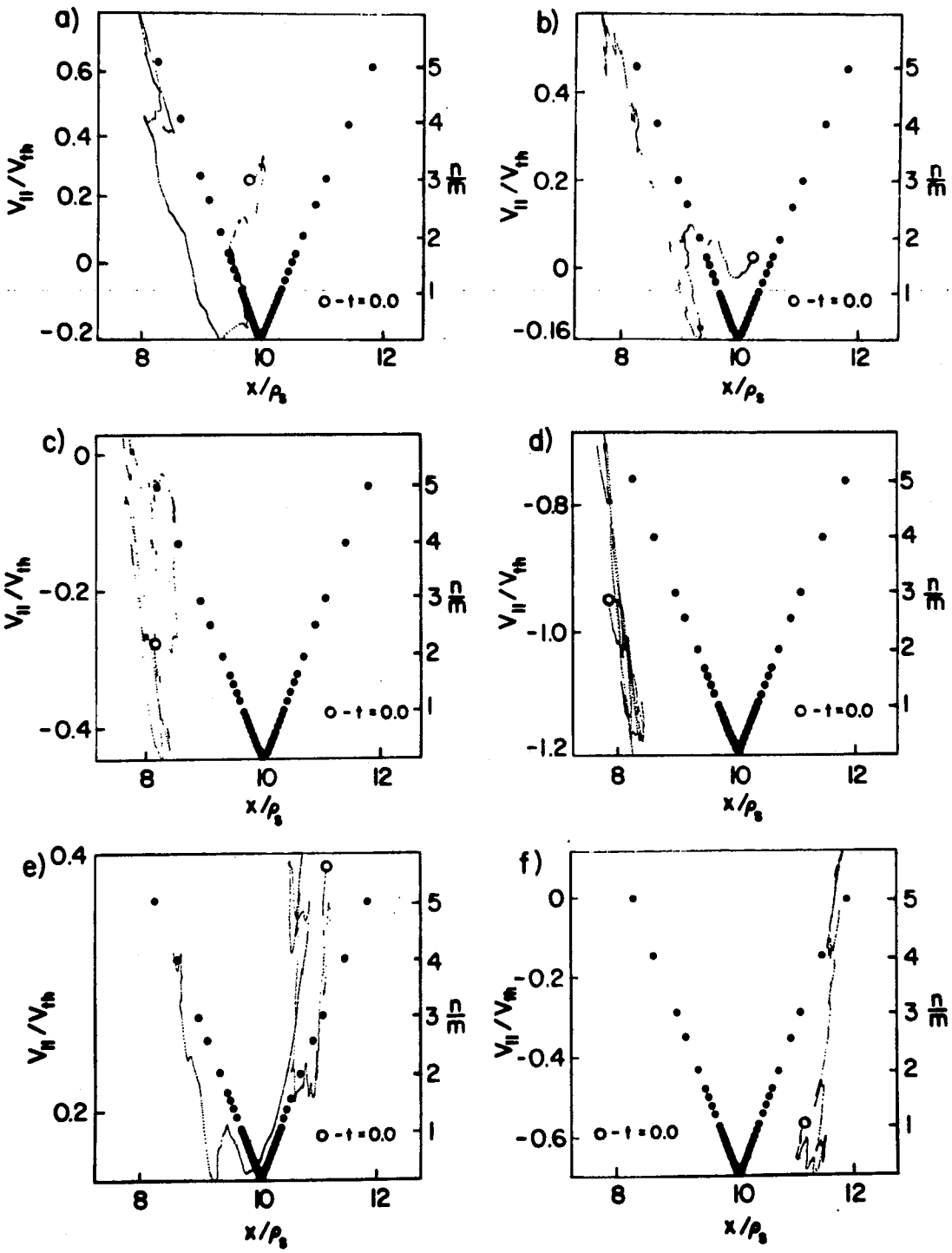

Fig. 5

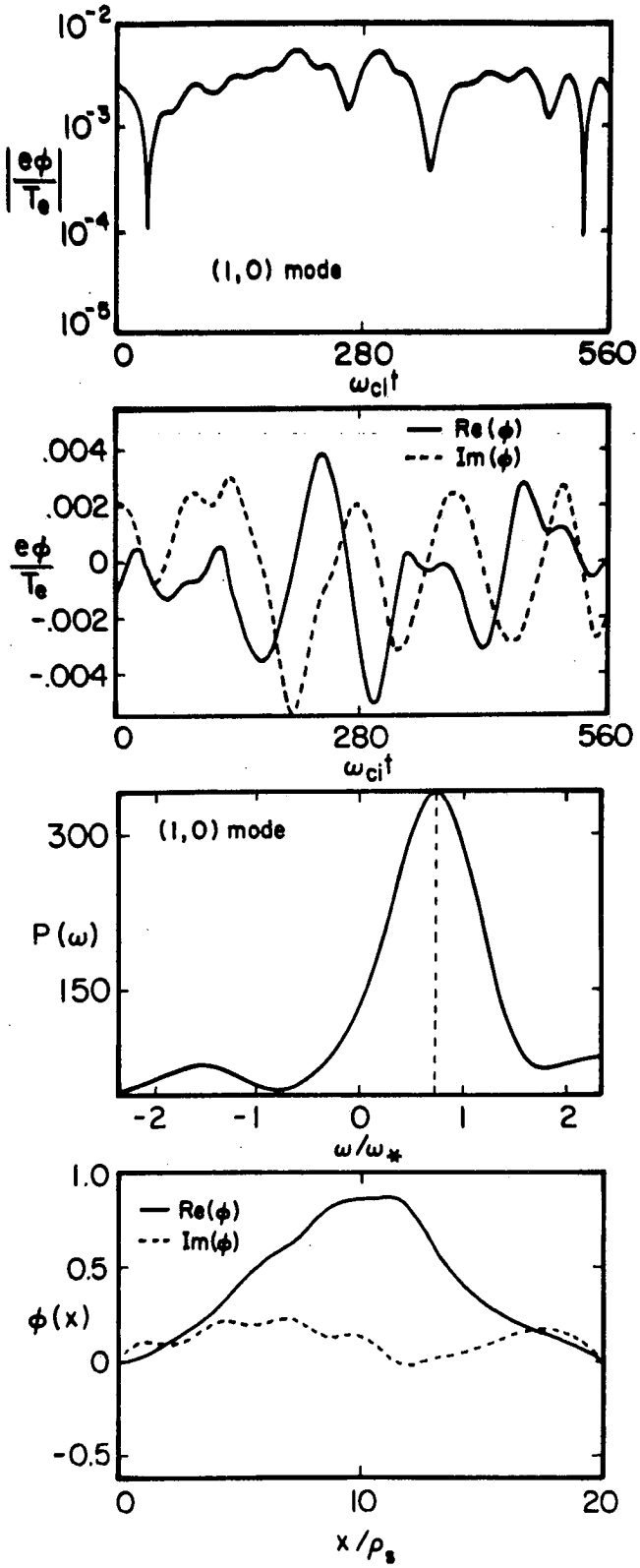
10^{-2}
10^{-3}
$\left|\frac{e\phi}{T_e}\right|$
10^{-4}
(1,0) mode
10^{-5}
0
280
560
$\omega_{ci}t$
Re(φ)
Im(φ)
.004
.002
$\frac{e\phi}{T_e}$
0
-.002
-.004
0
280
560
$\omega_{ci}t$
300
(1,0) mode
P(ω)
150
-2
-1
0
1
2
ω/ω_*
1.0
Re(φ)
Im(φ)
0.5
φ(x)
0
-0.5
0
10
20
x/ρ_s

Fig. 6